LARGE SCALE UNDERGROUND DETECTORS IN EUROPE* **

S.K. Katsanevas

IN2P3/CNRS
3 Rue Michel Ange, 75016 Paris, France

(Received June 14, 2006)

The physics potential and the complementarity of the large scale underground European detectors: Water Čerenkov (MEMPHYS), Liquid Argon TPC (GLACIER) and Liquid Scintillator (LENA) is presented with emphasis on the major physics opportunities, namely proton decay, supernova detection and neutrino parameter determination using accelerator beams.

PACS numbers: 14.60.Pq, 12.10.Dm, 97.60.Bw, 29.40.Ka

1. Introduction

There is a steady 25 year long tradition of large underground detectors, having produced an incredibly rich harvest of seminal discoveries. The pioneer Water Čerenkov detectors (IMB, Kamiokande, HPW) were built in the 80's to look for nucleon decay, a prediction of Grand Unified Theories. They fulfilled indeed this purpose by extending the proton decay lifetime limits by a few orders of magnitude. But their greatest achievement was that, by a serendipitous turn, as it often happens in physics, they have inaugurated: (a) particle astrophysics through the detection of neutrinos coming from the explosion of the Supernova 1987a [1–4] acknowledged by the Nobel prize for Koshiba and (b) the golden era of neutrino mass and oscillations by discovering indices of atmospheric oscillations and confirming earlier indices of solar neutrino oscillations [5–8] (Kamioka, SuperKamioka, SNO), later confirmed by man-made neutrinos, *i.e.* in the K2K experiment [9], KAMLAND [10], and most recently MINOS [11].

* Presented at the Cracow Epiphany Conference on Neutrinos and Dark Matter, Cracow, Poland, 5–8 January 2006.

** Largely based on a document edited by J.E. Campagne, A. Bueno, T.M. Undagoitia, M. Wurm and L. Oberauer representing GLACIER, LENA and MEMPHYS Collaborations, including theory contributions by A. Mirizzi and P. Fileviez-Perez.

The proposed detectors GLACIER[1] [12], LENA[2] [13, 14] and MEMPHYS[3] [15], intend to continue this rich legacy and by using complementary techniques hope to enlarge the discovery potential on several domains:

- They promise to extend the proton decay sensitivity by an order of magnitude.
- They can provide a detailed snapshot of the interior of a supernova explosion, while at the same time providing information on the neutrino mass matrix.
- They can probe the cosmologically important star formation rate through the cumulative supernova diffuse neutrino spectrum.
- They can increase our understanding of the neutrino mass matrix through a high statistics study of the atmospheric neutrino spectrum
- They can also increase our understanding of the solar interior with a high statistics study of the solar neutrino spectrum
- They can increase our understanding of the earth interior by the study of geoneutrinos (when far from man-made reactors) or inversely further the knowledge of the neutrino oscillation parameters using reactor neutrinos
- They could detect neutrinos of medium energy of astrophysical origin and also be sensitive to indirect decays of dark matter

The next section describes these detectors in some detail.

2. Brief detector description

The three detector design parameters are listed in Table I. They have in common their large mass, extrapolating by a factor of 20 to 50 with respect to previous installations, the need of large underground excavation presenting engineering challenges and a more or less acute dependence on large area photodetection. The most salient features of the detectors are discussed in the following sections.

[1] Giant Liquid Argon Charge Imaging ExpeRiment.
[2] Low Energy Neutrino Astronomy.
[3] MEgaton Mass PHYSics.

2.1. Liquid argon TPC

GLACIER (Fig. 1) is the extrapolation up to 100 kT of a Liquid Argon Time Projection Chamber. A summary of parameters are listed in Table I. For the purpose of this presentation the detector can be subdivided into two parts: (1) the liquid argon tanker and (2) the inner detector instrumentation.

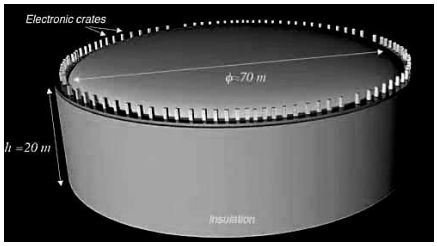

Fig. 1. An artistic view of a 100 kton single tanker liquid argon detector. The electronic crates are located at the top of the dewar.

TABLE I

Some basic parameters of the three detector baseline designs.

	GLACIER	**LENA**	**MEMPHYS**
dimensions			
type	vertical cylinder	horizontal cylinder	$3 \div 5$ shafts
diam. $\times$ length	$\phi = 70\text{m} \times H = 20\text{m}$	$\phi = 30\text{m} \times L = 100\text{m}$	($\phi = 65\text{m} \times H = 65\text{m}$)
Mass (kt)	100	50	$440 \div 730$
Active target and readout			
type of target	liquid argon (boiling)	phenyl-o-xylyethane	water (option: 0.2% $GdCl_3$)
readout type	81,000 12" PMTs $\sim 30\%$ coverage		
	e^- drift 2 views 10^5 channels Č light 27,000 8" PMTs, $\sim 20\%$ coverage Scint. light 1,000 8" PMTs	12,000 20" PMTs $\gtrsim 20\%$ coverage	81,000 12" PMTs $\sim 30\%$ coverage

The basic design parameters can be summarized as follows:

1. Single 100 kton "boiling" cryogenic tanker with argon refrigeration (the cooling is done directly with argon, *e.g.* without nitrogen).

2. Charge imaging + scintillation + Čerenkov light readout for complete event information.

3. Charge amplification to allow for extremely long drifts: the detector is running in bi-phase mode. In view of the charge attenuation during the long (≈ 20 m) drift one needs to compensate with charge amplification near the anodes located in gas phase.

4. Possibility of adding a magnetic field.

The inner detector instrumentation is made of: a cathode, located near the bottom of the tanker, set at -2 MV creating a drift electric field of 1 kV/cm over the distance of 20 m. In this field configuration ionization electrons are moving upwards while ions are going downward. The electric field is delimited on the sides of the tanker by a series of ring electrodes (race-tracks) at the appropriate voltages (voltage divider).

The tanker contains both liquid and gas argon phases at equilibrium. Since purity is a concern for very long drifts of the order of 20 meters, the inner detector will be operated in bi-phase mode, namely drift electrons produced in the liquid phase are extracted from the liquid into the gas phase with the help of an appropriate electric field. The GLACIER measurements show that the threshold for 100% efficient extraction is about 3 kV/cm. Hence, just below and above the liquid two grids define the liquid extraction field. In addition to charge readout, there will be PMTs around the tanker. Scintillation and Čerenkov light can be readout essentially independently [16]. In order to be sensitive to DUV scintillation, the PMTs are coated with a wavelength shifter (Tetraphenyl-Butadiene).

About 1000 immersed phototubes with WLS would be used to identify the (isotropic and bright) scintillation light. While about 27000 immersed $8''$-phototubes without WLS would provide a 20% coverage of the surface of the detector would count the Čerenkov photons; the should have single photon counting capabilities.

2.2. Liquid scintillator

The LENA detector is planned to have a cylindrical shape with about 100 m length and 30 m diameter (Fig. 2 and Table I). An inside part of 13 m radius will contain approximately 50 kt of liquid scintillator while the outside part will be filled with water to act as a muon veto. A fiducial

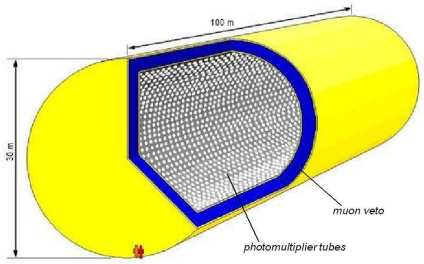

Fig. 2. Sketch of the LENA detector.

volume for proton decay will be defined having a radius of 12 m. About 12 000 photomultipliers of 50 cm diameter each, covering about 30% of the surface, will collect the light produced by the scintillator. PXE (phenyl-o-xylylethane) is foreseen as scintillator solvent because of its high light yield and its safe handling procedures. The optical properties of a liquid scintillator based on PXE have been investigated in the Counting Test Facility (CTF) for BOREXINO at the Gran Sasso underground laboratory [17]. A yield of 372 $\pm$ 8 photoelectrons per MeV (pe/MeV) have been measured in this experiment with an optical coverage of 20%. The attenuation length of $\sim$ 3 m (at 430 nm) was substantially increased to $\sim$ 12 m purging the liquid in a weak acidic alumina column [17]. With these values an expected photoelectron yield of $\sim$ 120 pe/MeV can be estimated for events in the center of the LENA detector. Currently the optical properties of mixtures of PXE and derivatives of mineral oils are under investigation [18].

2.3. Water Čerenkov

The MEMPHYS detector (Fig. 3) is an extrapolation of Super-Kamiokande up to 730 kT. This Water Čerenkov detector is a collection of up to 5 shafts, though 3 are enough for a nominal 440 kt fiducial mass used for the evaluation of its physics potential. Each shaft is 65 m in diameter and 65 m height for the total water container dimensions, representing an extrapolation by a factor 4 with respect to the Super-Kamiokande running detector. The PMT surface located at 2 m inside the water container is covered by about 81,000 12" PMTs to reach a 30% surface coverage equivalent to a 40% coverage with 20" PMTs. The fiducial volume is defined by an additional conservative guard of 2 m. The outer volume between the PMT surface and the water vessel is instrumented with 8" PMTs. In the US and in Japan, UNO [19] and Hyper-Kamiokande [20] respectively, are similar in many respects and the presented physics potential may be transposed also for those detectors. In the following, except when contrary mentioned, the Super-Kamiokande analysis is used to compute the physics potential.

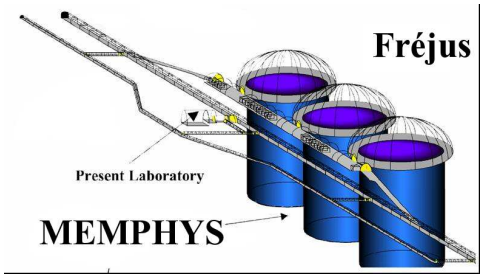

Fig. 3. Sketch of the MEMPHYS detector under the Fréjus mountain (Europe).

There is also a very promising R&D activity concerning the possibility to fill the Water Čerenkov with Gadolinium salt ($GdCl_3$) in order to decrease the background in many physics channels by tagging the neutron produced in the inverse beta decay interaction of $\bar{\nu}_e$ on free protons. For instance, 100 tons of $GdCl_3$ in Super-Kamiokande would yield more then 90% neutron captures on Gd [21]. The site located in the Fréjus mountain in the Alps, which is crossed by a road-tunnel connecting France (Modane) to Italy (Bardonecchia), has a number of interesting characteristics, namely its great depth, the good quality of the rock, the fact that it offers horizontal access, its distance from CERN (130 km) near optimal for neutrino oscillation studies, the opportunity of the planned excavation circa 2010 of a second tunnel for safety purposes.

DSM (CEA) and IN2P3 (CNRS) performed a feasibility study of a Large Underground Laboratory in the central region of the Fréjus tunnel, near the already existing LSM Laboratory. This preliminary study, performed by the companies that made the study and managed the realization of the Fréjus road tunnel and of the Laboratoire Souterrain de Modane (LSM), used a large number of measurements of the rock characteristics, in order to determine the most favorable regions along the road tunnel and to constrain the simulations of the present pre-study for the Large Laboratory.

The results of this preliminary study can be summarized as follows :

1. the best site (rock quality) is found in the middle of the mountain, at a depth of 4800 m.w.e (vertical depth) near the present laboratory;

2. of the two considered shapes : “tunnel” and “shaft”, the “shaft shape” is strongly preferred;

3. cylindrical shafts are feasible up to a diameter $\Phi = 65$ m and a full height $h = 80$ m (~ 250000 m^3).

Up to five shafts, of about 250000 m^3 each, can be located between the road tunnel and the railway tunnel. Three shafts of 250000 m^3 each would have a fiducial mass of 440 kton ("UNO-like" scenario). Smaller shafts could be excavated for *e.g.* a Liquid Argon detector.

3. A selection of science drivers

I briefly review here the performances of the 3 types of detector in what concerns proton decay, supernova and beam related neutrino oscillation physics. Other physics topics accessible to large underground detectors, as for instance solar and atmospheric neutrinos, indirect dark matter searches geoneutrinos and reactor neutrinos will be reported in a forthcoming white paper authored by researchers in the three collaborations.

3.1. Proton decay sensitivity

For all relevant aspects of the proton stability in grand unified theories, in strings and in branes see reference [22]. Since proton decay is the most dramatic prediction coming from theories where the matter is unified, one hopes to test those scenarios at future experiments.

Most of the models (Supersymmetric or non-Supersymmetric) predict a lifetime τ_p below ranging from 10^{33} years to 10^{37} years. The most common model predictions are listed in Table II.

TABLE II

Summary of some recent predictions on proton partial lifetimes.

Model	Decay modes	Prediction	References
Georgi–Glashow model	—	ruled out	[24]
Minimal realistic non-SUSY SU(5)	all channels	$\tau_p^{\text{upper}} = 1.4 \times 10^{36}$	[25]
Two Step Non-SUSY SO(10)	$p \to e^+\pi^0$	$\approx 10^{33-38}$	[26]
Minimal SUSY SU(5)	$p \to \bar{\nu}K^+$	$\approx 10^{32-34}$	[27]
SUSY SO(10) with 10_H, and 126_H	$p \to \bar{\nu}K^+$	$\approx 10^{33-36}$	[28]
M-Theory(G_2)	$p \to e^+\pi^0$	$\approx 10^{33-37}$	[29]

3.1.1. Simulation for proton decay

Due to its excellent imaging and energy resolution, GLACIER has the potentiality to discover nucleon decay in an essentially background-free environment. To understand the potential background contamination for this kind of search, the GLACIER team has carried out a detailed simulation

of nucleon decays in argon, *i.e.* including final state nuclear effects. Atmospheric neutrino and cosmic muon induced backgrounds have been fully simulated as well.

In order to quantitatively estimate the potential of the LENA detector for measuring the proton lifetime, a Monte Carlo simulation for the decay channel $p \to K^+\overline{\nu}$ has been performed. For this purpose, the Geant4 simulation toolkit has been used [30]. Not only all default Geant4 physics lists were included but also optical processes as scintillation, Čerenkov light production, Rayleigh scattering and light absorption. From these simulations a light yield of ~ 110 pe/MeV for an event in the center of the detector has been estimated.

No specific simulation for MEMPHYS has been carried out yet. They therefore rely on the study done by UNO [19], adapting the results to MEMPHYS.

3.1.2. $p \to e^+\pi^0$

Following UNO study, the detection efficiency of $p \to e^+\pi^0$ (3 showering rings event) is $\epsilon = 43\%$ for a 20 inch-PMT coverage of 40% or its equivalent. The corresponding estimated atmospheric neutrino induced background is at the level of 2.25 events/Mt yr. From these efficiencies and background levels, proton decay sensitivity as a function of detector exposure can be estimated. A 10^{35} years partial lifetime (τ_p/B) could be reached at the 90% C.L. for a 5 Mt yr exposure (10 yrs) with MEMPHYS (similar to case A in Fig. 4). Beyond that exposure, tighter cuts may be envisaged to further reduce the atmospheric neutrino background to 0.15 events/Mt yr, by selecting quasi exclusively the free proton decays.

The positron and the two photons issued from the π^0 gives clear events in the GLACIER detector. They find that the π^0 is absorbed by the nucleus $\sim$45% of the times. Assuming a perfect particle and track identification, one may expect a 45% efficiency and a background level of 1 event/Mt yr. So, for a 1 Mt yr (10 yrs) exposure with GLACIER one reaches $\tau_p/B > 0.5\times10^{35}$ yrs at 90% C.L. (see Fig. 6).

In a liquid scintillator detector the decay $p \to e^+\pi^0$ will produce an ~ 938 MeV signal coming from e^+ and π^0 showers. Only atmospheric neutrinos are expected to cause background events in this energy range. Using the fact that showers from both e^+ and π^0 propagate $\sim$4 m in opposite directions before being stopped, atmospheric neutrino background can be reduced. Preliminary estimates show that the current limit for this channel ($\tau_p/B = 5.4 \times 10^{33}$ yrs [31]) could be improved with LENA.

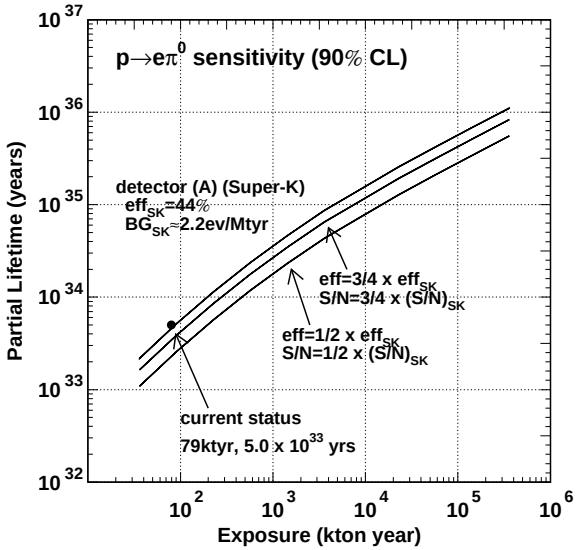

Fig. 4. Sensitivity for $e^+\pi^0$ proton decay lifetime, as determined by UNO [19]. MEMPHYS corresponds to case (A).

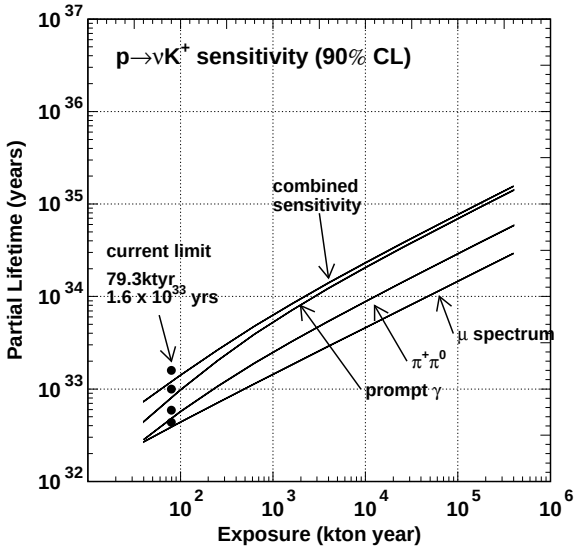

Fig. 5. Expected sensitivity on νK^+ proton decay as a function of MEMPHYS exposure [19] (see text for details).

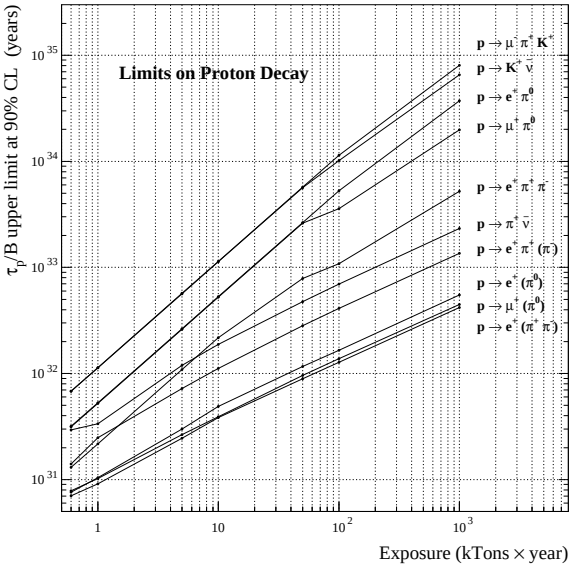

Fig. 6. Expected proton decay lifetime limits (τ/B at 90% C.L.) as a function of exposure for GLACIER.

3.1.3. $p \to \overline{\nu} K^+$

In LENA, proton decay events via the mode $p \to K^+ \overline{\nu}$ have a very clear signature. The kaon causes a prompt monoenergetic signal ($T = 105$ MeV) and from the kaon decay there is a short-delayed second monoenergetic signal, bigger than the first one. The kaon has a lifetime of $\tau(K^+) = 12.8$ ns and two main decay channels: with a probability of 63.43 % it decays via $K^+ \to \mu^+ \nu_\mu$ and with 21.13%, via $K^+ \to \pi^+ \pi^0$.

Simulations of proton decay events and atmospheric neutrino background has been performed and a pulse shape analysis has been applied. From the analysis an efficiency of 65% for the detection of a possible proton decay has been determined and a background suppression of $\sim 2 \times 10^4$ has been achieved [14]. A detail study of background implying pion and kaon production in atmospheric neutrino reactions has been performed leading to a background rate of 0.064 y^{-1} due to the reaction $\nu_\mu + p \to \mu^- + K^+ + p$.

For the current proton lifetime limit for the channel considered ($\tau_p/B = 2.3 \times 10^{33}$ yrs) [32], about 40.7 proton decay events would be observed in LENA after a measuring time of ten years with less than 1 background event. If no signal is seen in the detector within ten years, the lower limit for the lifetime of the proton will be placed at $\tau_p/B > 4 \times 10^{34}$ yrs at 90% C.L.

GLACIER uses dE/dx versus range as discriminating variable in a Neural Net to obtain the particle identity. They expect less than 1% of kaons mis-identified as protons. In this channel, the selection efficiency is high (97%) for a low background < 1 event/Mt yr. In case of absence of signal, they expect to reach $\tau_p/B > 1.1 \times 10^{35}$ yrs at 90% C.L. for 1 Mt yr (10 years) exposure (see Fig. 6).

For the MEMPHYS detector, one should rely on the detection of the decay products of the K^+ since its momentum (360 MeV) is below the water Čerenkov threshold (*i.e.* 570 MeV): a 256 MeV/c muon and its decay electron (type I) or a 205 MeV/c π^+ and π^0 (type II), with the possibility of a delayed (12 ns) coincidence with the 6 MeV ^{15}N de-excitation prompt γ (Type III). Using the imaging and timing capability of Super-Kamiokande, the efficiency for the reconstruction of $p \to \overline{\nu} K^+$ is $\epsilon = 33\%$ (I), 6.8% (II) and 8.8% (III), and the background is at 2100, 22 and 6 events/Mt yr level. For the prompt γ method, the background is dominated by mis-reconstruction. As stated by UNO, there are good reasons to believe that this background can be lowered by at least a factor 2 corresponding to the atmospheric neutrino interaction $\nu p \to \nu \Lambda K^+$. In these conditions, and using Super-Kamiokande performances, a 5 Mt yr MEMPHYS exposure would allow to reach $\tau_p/B > 2 \times 10^{34}$ yrs (see Fig. 5).

3.1.4. Comparison between the detectors

Preliminary comparisons have been done between the detectors (Table III). For the $e^+\pi^0$ channel, the Čerenkov detector gets a better limit due to its higher mass. However it should be noted that GLACIER, although five times smaller in mass than MEMPHYS, gets an expected limit that is only a factor two smaller. Liquid argon TPCs and liquid scintillator detectors get better results for the $\bar{\nu} K^+$ channel, due to their higher detection efficiency. The two techniques look therefore quite complementary and it would be worth to investigate deeper the pros and cons of each techniques with other channels not yet addressed by the present study as $e^+(\mu^+) + \gamma$ and neutron decays.

3.2. Supernova neutrinos

A supernova (SN) neutrino detection represents one of the frontiers of neutrino astrophysics. It will provide invaluable information on the astrophysics of the core-collapse explosion phenomenon and on the neutrino mixing parameters. In particular, neutrino flavor transitions in the SN envelope are sensitive to the value of θ_{13} and the type of mass hierarchy. The detection of SN neutrino spectra at Earth can significantly contribute to sharpen our understanding of these unknown neutrino parameters. On the other hand, a detailed measurement of the neutrino signal from a galactic SN could yield important clues on the SN explosion mechanism.

TABLE III

Summary of the $e^+\pi^0$ and $\bar{\nu}K^+$ discovery potential by the three detectors. The $e^+\pi^0$ channel is not yet simulated in LENA.

	GLACIER	LENA	MEMPHYS
$e^+\pi^0$			
$\epsilon(\%)$/Bkgd(Mt yr)	45/1	—	43/2.25
τ_p/B (90% C.L., 10 yrs)	0.5×10^{35}	—	1.0×10^{35}
$\bar{\nu}K^+$			
$\epsilon(\%)$/Bkgd(Mt yr)	97/1	65/1	8.8/3
τ_p/B (90% C.L., 10 yrs)	1.1×10^{35}	0.4×10^{35}	0.2×10^{35}

3.2.1. SN neutrino emission and oscillations

A core-collapse supernova marks the evolutionary end of a massive star ($M \gtrsim 8\,M_\odot$) which, at the end of its life, collapses and ejects its outer mantle in a shock-wave driven explosion. The collapse to a neutron star or a black hole liberates a gravitational binding energy, $E_{\rm B} \approx 3 \times 10^{53}$ erg, released at $\sim 99\%$ into neutrinos (and antineutrinos) of all flavors, and only at $\sim$1% into the kinetic energy of the explosion.

In general, numerical simulations of supernova explosions provide the original neutrino spectra in energy and time F^0_ν. Such initial distributions are modified by flavor transitions in SN envelope, in vacuum (and eventually in Earth matter).

$$F^0_\nu \longrightarrow F_\nu\,. \tag{1}$$

Regarding the initial neutrino distributions F^0_ν, a SN collapsing core is roughly a black-body source of thermal neutrinos, emitted on a timescale of $\sim$ 10 s. Energy spectra parametrization are typically cast in the form of quasi-thermal distributions, with average energies: $\langle E_{\nu_e}\rangle = 9 - 12$ MeV, $\langle E_{\bar{\nu}_e}\rangle = 14 - 17$ MeV, $\langle E_{\nu_x}\rangle = 18 - 22$ MeV, where ν_x indicates any non-electron flavor.

The oscillated neutrino fluxes arriving at Earth may be written in terms of the energy-dependent "survival probability" p ($\bar{p}$) for neutrinos (antineutrinos) as [33]

$$\begin{aligned} F_{\nu_e} &= pF^0_{\nu_e} + (1-p)F^0_{\nu_x}\,, \\ F_{\bar{\nu}_e} &= \bar{p}F^0_{\bar{\nu}_e} + (1-\bar{p})F^0_{\nu_x}\,, \\ 4F_{\nu_x} &= (1-p)F^0_{\nu_e} + (1-\bar{p})F^0_{\bar{\nu}_e} + (2+p+\bar{p})F^0_{\nu_x}\,, \end{aligned} \tag{2}$$

where ν_x stands for either ν_μ or ν_τ. The probabilities p and $\bar{p}$ crucially depend on the neutrino mass hierarchy and on the unknown value of the mixing angle θ_{13} as shown in Table IV.

TABLE IV

Values of the p and $\bar{p}$ parameters used in Eq. (2) in different scenario of mass hierarchy and $\sin^2\theta_{13}$.

Mass hierarchy	$\sin^2\theta_{13}$	p	$\bar{p}$
Normal	$\gtrsim 10^{-3}$	0	$\cos^2\theta_{12}$
Inverted	$\gtrsim 10^{-3}$	$\sin^2\theta_{12}$	0
Any	$\lesssim 10^{-5}$	$\sin^2\theta_{12}$	$\cos^2\theta_{12}$

3.2.2. SN neutrino detection

Galactic core-collapse supernovae are rare, perhaps a few per century. Up to now, supernova neutrinos have been measured only once during SN 1987A explosion in the Large Magellanic Cloud ($d = 50$ kpc). Due to the relatively small masses of the detectors operating at that time, only few events were detected (11 in Kamiokande [1, 2] and 8 in IMB [3, 4]). The three proposed large-volume neutrino detectors with a broad range of science goals might guarantee continuous exposure for several decades, so that a high-statistics supernova neutrino signal may eventually be observed.

Expected number of events for GLACIER, MEMPHYS and LENA are reported in Table V, for a typical galactic SN distance of 10 kpc. In the upper panel it is reported the total number of events, while the lower part refers to the ν_e signal detected during the prompt neutronization burst, with a duration of ~ 25 ms, just after the core bounce.

One sees that $\bar{\nu}_e$ detection by Inverse β Decay is the golden channel for MEMPHYS, although the ν_e channel can be measured by the elastic scattering reaction $\nu_x + e^- \to e^- + \nu_x$ [37].

The Inverse β Decay is also a golden channel for LENA. In addition, the electron neutrino signal can be detected thanks to the interaction on ^{12}C. The three charged current reactions will deliver information on ν_e and $\bar{\nu}_e$ fluxes and spectra while the three neutral current reactions, sensitive to all neutrino flavors will provide information on the total flux.

GLACIER has also the opportunity to see the ν_e by charged current interactions on ^{40}Ar with a very low threshold, permitting a signal with obtain good statistics from the neutronization burst. Using its unique features look at ν_e CC it is possible to probe oscillation physics during the early stage of the SN explosion, and using the NC it is possible to decouple the SN mechanism from the oscillation physics [38, 39].

The detection complementarity between ν_e and $\bar{\nu}_e$ is of great interest and would assure a unique way to probe SN explosion mechanism as well as neutrino intrinsic properties. Moreover, the huge statistics would allow spectral studies in time and in energy domain.

TABLE V

Summary of the expected neutrino interaction rates in the different detectors for a $8M_{\odot}$ SN located at 10 kpc (Galactic center). The following notations have been used: IβD, eES and pES stands for Inverse β Decay, electron and proton Elastic Scattering, respectively. The final state nuclei are generally unstable and decay either radiatively (notation *), or by β^-/β^+ weak interaction (notation $^{\beta^-,^+}$). The rates of the different reaction channels are listed, and for LENA they have been obtained by scaling the predicted rates from [34, 35].

MEMPHYS		LENA		GLACIER	
Interaction	Rates	Interaction	Rates	Interaction	Rates
$\bar{\nu}_e$ IβD	2×10^5	$\bar{\nu}_e$ IβD	9×10^3	$\nu_e^{\rm CC}(^{40}{\rm Ar}, ^{40}K^*)$	2.5×10^4
$\overset{(-)}{\nu}{}_e^{\rm CC}(^{16}{\rm O}, X)$	10^4	ν_x pES	7×10^3	$\nu_x^{\rm NC}(^{40}{\rm Ar}^*)$	3.0×10^4
ν_x eES	10^3	$\nu_x^{\rm NC}(^{12}{\rm C}^*)$	3×10^3	ν_x eES	10^3
		ν_x eES	600	$\bar{\nu}_e^{\rm CC}(^{40}{\rm Ar}, ^{40}{\rm Cl}^*)$	540
		$\bar{\nu}_e^{\rm CC}(^{12}{\rm C}, ^{12}{\rm B}^{\beta^+})$	500		
		$\nu_e^{\rm CC}(^{12}{\rm C}, ^{12}{\rm N}^{\beta^-})$	85		
Neutronization burst rates					
MEMPHYS	60	ν_e eES			
LENA	~ 10	$\nu_e^{\rm CC}(^{12}{\rm C}, ^{12}{\rm N}^{\beta^-})$			
GLACIER	380	$\nu_x^{\rm NC}(^{40}{\rm Ar}^*)$			

It has been frequently stressed that it will be difficult to establish SN neutrino oscillation effects solely on the basis of a $\bar{\nu}_e$ or ν_e "spectral hardening" relative to theoretical expectations. Therefore, in the recent literature the importance of model-independent signatures has been emphasized. Here we focus mainly on the signatures associated to: the prompt ν_e neutronization burst, the shock-wave propagation and the Earth matter crossing.

The analysis of the time structure of the SN signal during the first few tens of milliseconds after the core bounce can provide a clean indication if the full ν_e burst is present or absent and therefore allows one to distinguish between different mixing scenarios as indicated by the third column of Table VI. For example, if the mass ordering is normal and the θ_{13} is large, the ν_e burst will fully oscillate into ν_x. If θ_{13} is measured in the laboratory to be large, for example by one of the forthcoming reactor experiments, then one may distinguish between the normal and inverted mass ordering.

A few seconds after core bounce, the SN shock wave will pass the density region in the stellar envelope relevant for oscillation matter effects, causing a transient modification of the survival probability and thus a time-dependent signature in the neutrino signal [40, 41]. It would show a characteristic dip when the shock wave passes [36], or a double-dip feature if a reverse shock

TABLE VI

Summary of the neutrino properties effect on ν_e and $\bar{\nu}_e$ signals.

Mass hierarchy	$\sin^2\theta_{13}$	ν_e neutronization peak	Shock wave	Earth effect
Normal	$\gtrsim 10^{-3}$	Absent	ν_e	$\bar{\nu}_e$ ν_e (delayed)
Inverted	$\gtrsim 10^{-3}$	Present	$\bar{\nu}_e$	ν_e $\bar{\nu}_e$ (delayed)
Any	$\lesssim 10^{-5}$	Present	—	both $\bar{\nu}_e$ ν_e

occurs [42]. The detectability of such a signature has been studied in a Megaton Water Čerenkov detector like MEMPHYS by the IβD [36], and in a Large liquid argon detector like GLACIER by Ar CC interactions [43]. The shock wave effects would be certainly visible also in a large volume scintillator like LENA. Of course, apart from identifying the neutrino mixing scenario, such observations would test our theoretical understanding of the core-collapse SN phenomenon.

One unequivocal indication of oscillation effects would be the energy-dependent modulation of the survival probability $p(E)$ caused by Earth matter effects [44]. The Earth matter effects can be revealed by wiggles in energy spectra and LENA benefit from a better energy resolution than MEMPHYS in this respect which may be partially compensated by 10 times more statistics [45]. The Earth effect would show up in the $\bar{\nu}_e$ channel for the normal mass hierarchy, assuming that θ_{13} is large (Table VI). Another possibility to establish the presence of Earth effects is to use the signal from two detectors if one of them sees the SN shadowed by the Earth and the other not. A comparison between the signal normalization in the two detectors might reveal Earth effects [46]. The shock wave propagation can influence the Earth matter effect, producing a delayed effect 5–7 s after the core-bounce, in some particular situations [47] (Table VI).

Exploiting these three experimental signatures, by the joint efforts of the complementarity SN neutrino detection in MEMPHYS, LENA, and GLACIER it would be possible to extract valuable information on the neutrino mass hierarchy and to put a bound on θ_{13}, as shown in Table VI.

Other interesting ideas has been also studied in literature, ranging from the pointing of a SN by neutrinos [48], an early alert for SN observatory exploiting the neutrino signal [49], and the detection of neutrinos from the last phases of a burning star [50].

Up to now, we have investigated SN in our Galaxy, but the calculated rate of supernova explosions within a distance of 10 Mpc is about 1 per year. Although the number of events from a single explosion at such large distances would be small, the signal could be separated from the background with the request to observe at least two events within a time window comparable to the neutrino emission time-scale ($\sim$ 10 sec), together with the full energy and time distribution of the events [51]. In a MEMPHYS detector, with at least two neutrinos observed, a supernova could be identified without optical confirmation, so that the start of the light curve could be forecasted by a few hours, along with a short list of probable host galaxies, providing thus a trigger for gravitational antennas and neutrino telescopes.

3.2.3. Diffuse Supernova Neutrino Background

A galactic Supernova explosion will be a spectacular source of neutrinos, so that a variety of neutrino and SN properties could be determined. However, only one such explosion is expected in 20 to 100 years. Alternatively, it has been suggested that we might detect the cumulative neutrino flux from all the past SN in the Universe, the so called Diffuse Supernova Neutrino Background (DSNB). In particular, there is an energy window around 20–40 MeV where the DSNB signal can emerge above other sources, so that proposed detectors may measure this flux after some years of exposure times.

The DSNB signal, although weak, is not only "guaranteed", but can also probe different physics from a galactic SN, including processes which occur on cosmological scales. For instance, the DSNB signal is sensitive to the evolution of the SN rate, which is closely related to the star formation rate [52, 56]. Additionally, neutrino decay scenarios with cosmological lifetimes could be analyzed and constrained [53], as proposed in [54].

An upper limit on the DSNB flux has been set by the Super-Kamiokande experiment [55]

$$\phi_{\bar{\nu}_e}^{\mathrm{DSNB}} < 1.2 \ \mathrm{cm}^{-2}\,\mathrm{s}^{-1}\,, \qquad (E_\nu > 19.3 \ \mathrm{MeV})\,. \tag{3}$$

However, most of the estimates are below this limit and therefore DSNB detection appears to be feasible only with the large detector foreseen, through $\bar{\nu}_e$ inverse beta decay in MEMPHYS and LENA detectors and through $\nu_e + {}^{40}\mathrm{Ar} \to e^- + {}^{40}\mathrm{K}^*$ (and the associated gamma cascade) in GLACIER [61].

Typical estimates for DSNB fluxes (see for example [56]) predict an event rate of the order of $(0.1 \div 0.5)$ cm^{-2} s^{-1} MeV^{-1} for energies above 20 MeV.

The DSNB signal energy window is constrained from above by the atmospheric neutrinos and from below by either the nuclear reactor $\bar{\nu}_e$ (I), the spallation production unstable radionuclei by cosmic ray muons (II), the decay of "invisible" muon into electron (III), and solar ν_e neutrinos (IV). The three detectors are affected differently from these backgrounds.

Namely, MEMPHYS filled with pure water is mainly affected by type III due to the fact that the muons may have not enough energy to produce Çerenkov light, while GLACIER looking at ν_e is mainly affected by type IV backgrounds. LENA takes benefit from the delayed neutron capture in $\bar{\nu}_e + p \rightarrow n + e^+$, so it is mainly affected by type I which imposes an underground site far from nuclear plants. For instance, if LENA is deployed at the Center for Underground Physics in Pyhäsalmi (CUPP, Finland), there will be an observational window from ~ 9.5 to 30 MeV that is almost free of background. The expected rates of signal and background are presented in Table VII.

As pointed out [36], the addition of Gadolinium [21] in MEMPHYS permits the detection of the captured neutron releasing 8 MeV gamma after of the order of 20 μs (10 times faster than in pure water). It would thus give the possibility to reject neutrinos other than $\bar{\nu}_e$ that is to say not only the "invisible" muon (type III) but also the spallation background (type II).

TABLE VII

DSNB expected rates. The larger numbers are computed with the present limit on the flux by SuperKamiokande Collaboration. The lower numbers are computed for typical models. The background coming from reactor plants have been computed for specific locations for MEMPHYS and LENA. For MEMPHYS, the SuperKamiokande background has been scaled by the exposure. More studies are needed to estimate the background at the new Fréjus laboratory.

Interaction	Exposure	Energy Window	Signal/Bkgd
1 shaft MEMPHYS + 0.2% Gd (with bkgd Kamioka)			
$\bar{\nu}_e + p \rightarrow n + e^+$ $n + \mathrm{Gd} \rightarrow \gamma$ (8 MeV, 20 μs)	0.7 Mt yr 5 yrs	[15–30] MeV	(43-109)/47
LENA at Pyhäsalmi			
$\bar{\nu}_e + p \rightarrow n + e^+$ $n + p \rightarrow d + \gamma$ (2 MeV, 200 μs)	0.4 Mt yr 10 yrs	[9.5–30] MeV	(20-230)/8
GLACIER			
$\nu_e + {}^{40}\mathrm{Ar} \rightarrow e^- + {}^{40}\mathrm{K}^*$	0.5 Mt yr 5 yrs	[16–40] MeV	(40–60)/30

According to DSNB models [56], using different SN simulations (groups LL [57], TBP [58] and KRJ [59]) for the prediction of the DSNB energy spectrum and flux 20 to 230 events are expected in LENA in 10 years. The

exact number mainly depends on the uncertainties of the Star Formation Rate (SFR) in the near universe. Signal rates corresponding to three different DSNB models and the background rates due to the reactor (I) and atmospheric neutrinos are shown in Fig. 7 for 10 years of measurement with LENA in CUPP.

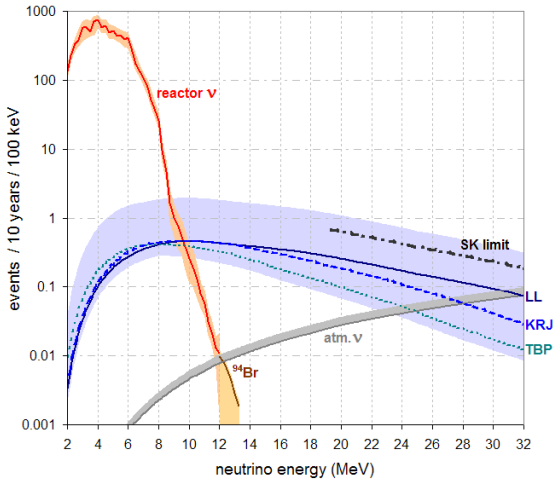

Fig. 7. Diffuse supernova neutrino signal and background in LENA detector in 10 years of exposure. Shaded regions give the uncertainties of all curves. An observational window between $\sim$ 9.5 to 30 MeV that is almost free of background can be identified.

Moreover, assuming the most likely rates of 2.8 to 5.5 DSNB events per year, after a decade of measurement statistics in LENA might already be good enough to distinguish between the LL and the TBP model that give the most different predictions on the DSNB's spectral slope and therefore event rates. This will give valuable constraints on the SN neutrino spectrum and explosion mechanism.

Further, if one achieves a threshold below 10 MeV for the DSN detection it might be possible to get a glimpse at the low-energetic part of the spectrum that is dominated by neutrinos emitted by SNe at redshifts $z > 1$. About 25% of the DSNB events in the observational window will be caused by these high-z neutrinos. This might provide a new way of measuring the SFR at high redshifts. At these distances, conventional astronomy looking for Star Formation Regions is strongly impeded by dust extinction of the UV light that is emitted by young stars. The z-sensitivity of the detector could be further improved by choosing a location far away from the nuclear power plants of the northern hemisphere. For instance, a near to optimum DSNB detection threshold of 8.4 MeV could be realized by deploying LENA in New Zealand.

An analysis of the expected DSNB spectrum that would be observed with a gadolinium-loaded Water Čerenkov detector has been carried out in [60]. The possible measurements of the parameters (integrated luminosity and average energy) of supernova $\bar{\nu}_e$ emission have been computed for 5 years running of a Gd-enhanced SuperKamiokande detector, which would correspond to 1 year of one Gd-enhanced MEMPHYS shaft. The results are shown in Fig. 8. Even if detailed studies on characterization of the background are needed, the DSNB events may be as powerful as the measurement made by Kamioka and IMB with the SN1987A $\bar{\nu}_e$ events.

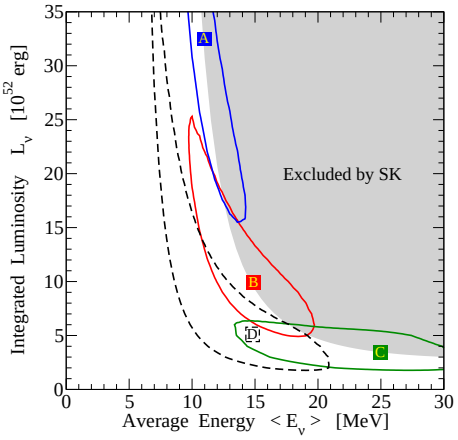

Fig. 8. Possible 90% C.L. measurements of the emission parameters of supernova electron antineutrino emission after 5 years running of a gadolinium-enhanced SK detector or 1 year of one gadolinium-enhanced MEMPHYS shaft [60].

3.3. Neutrinos from beams

This section reviews the physics program of the proposed detectors using different accelerator based neutrino beams attempting to measure the value of θ_{13}, the angle responsible for leptonic CP violation ($\delta_{\rm CP}$) and determine of the mass hierarchy (*i.e.* the sign of Δm^2_{31}) and this of the θ_{23} octant (*i.e.* $\theta_{23} > 45°$ or $\theta_{23} < 45°$).

In particular, the case of MEMPHYS at Fréjus using a projected new CERN 4MW proton driver (SPL) (a Super Beam option) and/or a possible new scheme of pure electron (anti)neutrino production by using radioactive ion decays (the βB Beam option) is presented. LENA is also considered as a candidate detector for the βB and some first elements of a work in progress are presented. Finally, the Neutrino Factory option (intense neutrino beams by mean of muon decays) can be well coupled to a LAr detector as large as GLACIER.

3.3.1. The CERN-SPL Super Beam

The CERN-SPL Super Beam project is a conventional neutrino beam although based on a 4MW SPL (Superconducting Proton Linac) proton driver impinging a liquid mercury target to generate an intense π^+ (π^-) beam with small contamination of kaon mesons. The initial baseline [62–66] has been improved [67] considering the specific requirements of a CERN to Fréjus baseline (130 km).

The use of a near and far detector will allow for both ν_μ disappearance and $\nu_\mu \to \nu_e$ appearance studies. The physics potential of the SPL Super Beam with MEMPHYS has been extensively studied [63,65,67–69]; however, the beam simulation will need some retuning after HARP results [70].

After 5 years exposure in ν_μ disappearance mode, a 3σ accuracy of (3–4)% can be achieved on Δm^2_{31}, and an accuracy of 22% (5%) on $\sin^2\theta_{23}$ if the true value is 0.5 (0.37) (Fig. 9). The use of atmospheric neutrinos (ATM) can alleviate the octant ambiguity in case of non-maximal mixing as it is shown in Fig. 9.

In appearance mode (2 years ν_μ plus 8 years $\bar{\nu}_\mu$), a 3σ discovery of non-zero θ_{13}, irrespective of the actual true value of $\delta_{\rm CP}$, is achieved for $\sin^2 2\theta_{13} \gtrsim 4 \times 10^{-3}$ ($\theta_{13} \gtrsim 3.6^\circ$) as shown in Fig. 10. For maximal CP violation ($\delta^{\rm true}_{\rm CP} = \pi/2, 3\pi/2$) the same discovery level can be achieved for $\sin^2 2\theta_{13} \gtrsim 8 \times 10^{-4}$ ($\theta_{13} \gtrsim 0.8^\circ$). The best sensitivity for testing CP violation (*i.e.* the data cannot be fitted with $\delta_{\rm CP} = 0$ nor $\delta_{\rm CP} = \pi$) is achieved for $\sin^2 2\theta_{13} \approx 10^{-2}$ ($\theta_{13} \approx 2.9^\circ$) where 75% of the possible value of $\delta_{\rm CP}$ can be tested at 3σ.

Although quite powerful, the SPL Super Beam is a conventional neutrino beam with known limitations due to (1) a lower production rate of anti-neutrinos compared to neutrinos which in addition to a smaller charged current cross-section impose to run 4 times longer in anti-neutrino modes; (2) the difficulty to setup a accurate beam simulation which implies to the design of a non-trivial near detector setup (*cf.* K2K, MINOS, T2K) to master the background levels. Thus, a new type of neutrino beam, the so-called betabeam (βB), is taken as a attractive alternative and is described in the following section as well as a combination of the two kinds of beams.

3.3.2. The CERN-βB baseline scenario

Beta beams have been proposed by Zucchelli in 2001 [72]. The idea is to generate pure, well collimated and intense $\nu_e(\bar{\nu}_e)$ beams by producing, collecting, accelerating radioactive ions and storing them in a decay ring in 10 ns long bunches, to suppress the atmospheric neutrino backgrounds. The resulting βB spectra can be easily computed knowing the beta decay spectrum of the parent ion and the Lorentz boost factor γ, and these beams

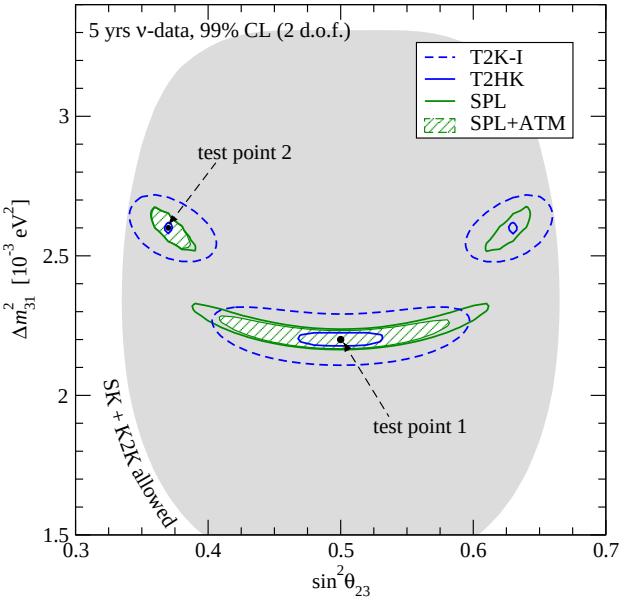

Fig. 9. Allowed regions of Δm^2_{31} and $\sin^2\theta_{23}$ at 99% C.L. (2 d.o.f.) after 5 yrs of neutrino data taking for SPL, T2K phase I, T2HK, and the combination of SPL with 5 yrs of atmospheric neutrino data in the MEMPHYS detector. For the true parameter values we use $\Delta m^2_{31} = 2.2\,(2.6) \times 10^{-3}$ eV^2 and $\sin^2\theta_{23} = 0.5\,(0.37)$ for the test point 1 (2), and $\theta_{13} = 0$ and the solar parameters as: $\Delta m^2_{21} = 7.9 \times 10^{-5}$ eV^2, $\sin^2\theta_{12} = 0.3$. The shaded region corresponds to the 99% C.L. region from present SK and K2K data [71].

are virtually background free from other flavors. The best ion candidates so far are ^{18}Ne and ^{6}He for $\nu_e$and $\bar{\nu}_e$, respectively. A baseline study for the βB has been initiated at CERN, and is pursued in the context of the European FP6 design study for EURISOL.

The potential of such βB sent to MEMPHYS has been studied in the context of the baseline scenario, using reference fluxes of 5.8×10^{18} ^{6}He useful decays/year and 2.2×10^{18} ^{18}Ne decays/year, at $\gamma = 100$, corresponding to a reasonable estimate by experts in the field of the ultimately achievable fluxes. The corresponding performances have been recently reviewed in reference [68], updating earlier studies [73–76].

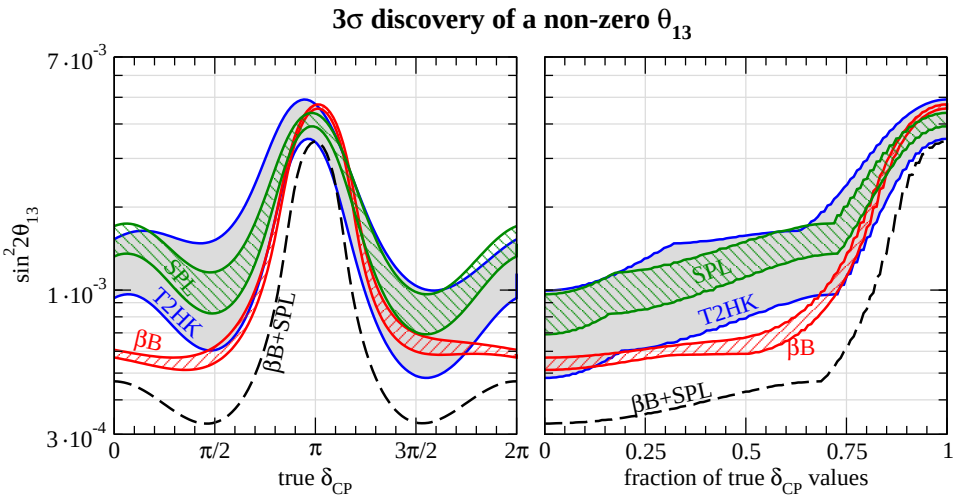

Fig. 10. 3σ discovery sensitivity to $\sin^2 2\theta_{13}$ for βB, SPL, and T2HK as a function of the true value of $\delta_{\rm CP}$ (left panel) and as a function of the fraction of all possible values of $\delta_{\rm CP}$ (right panel). The width of the bands corresponds to values for the systematical errors between 2% and 5%. The dashed curves correspond to the combination of βB and SPL with 10 yrs of total data taking each for a systematical error of 2%.

In Fig. 10 the result of running a βB during 10 years (5 years with neutrinos and 5 years with anti-neutrinos) is shown and proven to be better with respect to a SPL Super beam run, especially for maximal CP violation where a non-zero θ_{13} value can be stated at 3σ for $\sin^2 2\theta_{13} \gtrsim 6 \times 10^{-3}$ ($\theta_{13} \gtrsim 2.2°$). Moreover, it is worth noticing (Fig. 10) that the βB is less affected by systematic errors on the background compared to the SPL Super beam and T2HK.

LENA can as well be used as detector for a low-energy βB oscillation experiment. Using a neutrino beam of about 600–800 MeV, muon events are separable from electron events due to their different track lengths in the detector and due to the electron emitted in the muon decay after a mean time of 2.2 μs.

3.3.3. Combining SPL Beam and βB with MEMPHYS at Fréjus

Since a βB uses only a small fraction of the protons available from the SPL, Super and Beta beams can be run at the same time. Their combination leads to further improvements on the sensitivity on θ_{13} and $\delta_{\rm CP}$, as shown in Fig. 10. It increases especially at maximal CP violation the discovery potential down to $\sin^2 2\theta_{13} \gtrsim 3 \times 10^{-4}$ ($\theta_{13} \gtrsim 0.5°$).

Moreover, using only neutrino modes, ν_μ for SPL and ν_e for βB, if CPT symmetry is assumed, all the information can be obtained as $P_{\bar{\nu}_e \to \bar{\nu}_\mu} = P_{\nu_\mu \to \nu_e}$ and $P_{\bar{\nu}_\mu \to \bar{\nu}_e} = P_{\nu_e \to \nu_\mu}$. We illustrate this synergy in Fig. 11. In this scenario, time consuming anti-neutrino running can be avoided keeping the same physics discovery potential.

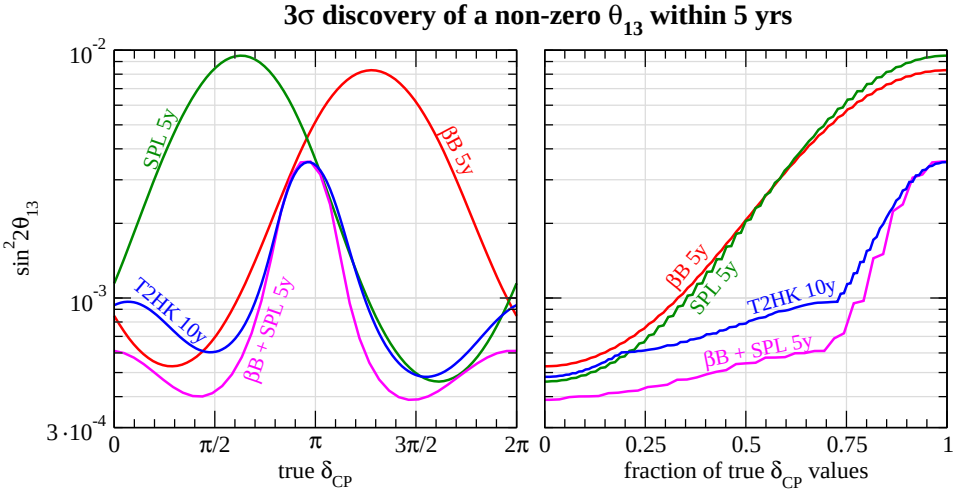

Fig. 11. Discovery potential of a finite value of $\sin^2 2\theta_{13}$ at 3σ ($\Delta\chi^2 > 9$) for 5 yrs neutrino data from βB, SPL, and the combination of βB + SPL compared to 10 yrs data from T2HK (2 yrs neutrinos + 8 yrs antineutrinos).

One can also combine SPL, βB and the atmospheric neutrinos (ATM) to alleviate the parameter degeneracies which lead to disconnected regions on the multi-dimensional space of oscillation parameters[4]. Atmospheric neutrinos, mainly multi-GeV e-like events, are also sensitive to the neutrino mass hierarchy if θ_{13} is sufficiently large due to Earth matter effects, whilst sub-GeV e-like events provide sensitivity to the octant of θ_{23} due to oscillations with Δm^2_{21}.

A feature of the ATM data is to provide a non-trivial sensitivity to the neutrino mass hierarchy (*i.e.* the sign of Δm^2_{31}) as shown in Fig. 12 for 10 years run. The mass hierarchy can be identified at 2σ C.L. provided $\sin^2 2\theta_{13} \gtrsim 0.02$ for βB and SPL combined [68].

Finally, it is worth mentioning that the combination of Super and β beams offers advantages, from the experimental point of view, since the same parameters θ_{13} and $\delta_{\rm CP}$ may be measured in many different ways, using 2 pairs of CP related channels, 2 pairs of T related channels, and 2 pairs of CPT related channels which should all give coherent results. In this

[4] See reference [77] for the definitions of *intrinsic*, *hierarchy*, and *octant* degeneracies.

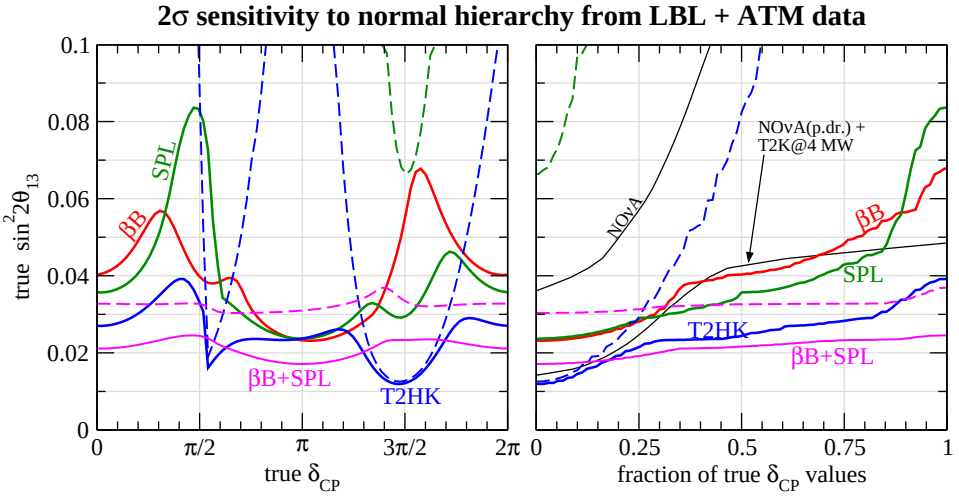

Fig. 12. Sensitivity to the mass hierarchy at 2σ ($\Delta\chi^2 = 4$) as a function of true values of $\sin^2 2\theta_{13}$ and $\delta_{\rm CP}$ (left), and the fraction of true values of $\delta_{\rm CP}$ (right). The solid curves are the sensitivities from the combination of long-baseline and atmospheric neutrino data, the dashed curves correspond to long-baseline data only. For comparison we show in the right panel also the sensitivities of NOνA and NOνA+T2K extracted from Fig. 13.14 of Ref. [78]. For the curve labeled "NOνA (p.dr.)+T2K@4 MW" a proton driver has been assumed for NOνA and the T2K beam has been up-graded to 4 MW, see Ref. [78] for details.

way the estimates of the systematic errors, different for each beam, will be experimentally cross-checked. And, needless to say, the unoscillated data for a given beam will give a large sample of events corresponding to the small searched-for signal with the other beam, adding more handles on the understanding of the detector response.

3.3.4. Neutrino Factory LAr detector

In order to fully address the oscillation processes at a neutrino factory, a detector should be capable of identifying and measuring all three charged lepton flavors produced in charged current interactions *and* of measuring their charges to discriminate the incoming neutrino helicity. This is an experimentally challenging task, given the required detector mass for long-baseline experiments.

The GLACIER concept offers a high granularity, excellent calorimetry non magnetized target detector, which provides a background free identification of electron neutrino charged current and a kinematical selection of tau neutrino charged current interactions. We can assume that charge dis-

crimination is available for muons reaching an external magnetized-Fe spectrometer. Another interesting and extremely challenging possibility would consist of magnetizing the whole liquid argon volume [86]. This set-up allows the clean classification of events into electron, right-sign muon, wrong-sign muon and no-lepton categories. In addition, high granularity permits a clean detection of quasi-elastic events, which by detecting the final state proton, provide a selection of the neutrino electron helicity without the need of an electron charge measurement.

Figure 13 shows the expected sensitivity in the measurement of the mixing angle between the first and the third family for a baseline of 7400 km. The maximal sensitivity to θ_{13} is achieved for very small background levels, since we are looking in this case for small signals; most of the information is coming from the clean wrong-sign muon class and from quasi-elastic events. On the other hand, if its value is not too small, for a measurement of θ_{13}, the signal/background ratio could be not so crucial, and also the other event classes can contribute to this measurement.

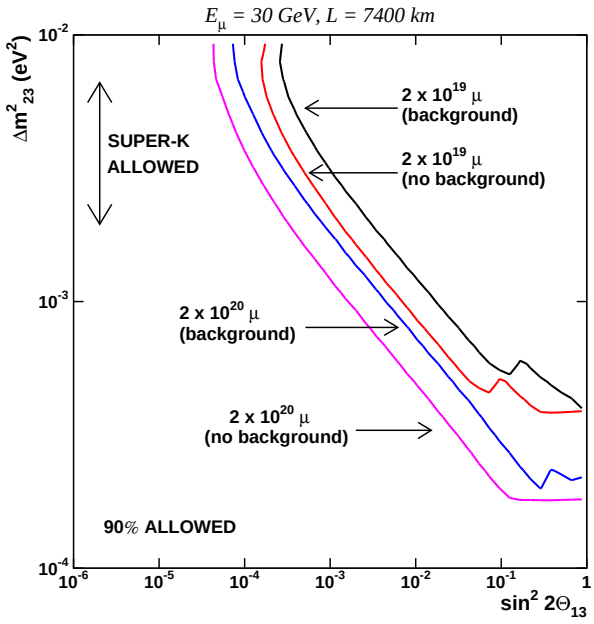

Fig. 13. GLACIER sensitivity for θ_{13}.

The study of CP violation in the lepton system is a very fascinating subject and probably, the most ambitious goal of an experiment at a neutrino factory. Matter effect can mimic CP violation; however, a multi parameter

fit at the right baseline can allow a simultaneous determination of matter and CP-violating parameters.

To detect CP violation effects, the most favorable choice of neutrino energy E_ν and baseline L is in the region of the "first maximum", given by $(L/E_\nu)^{\max} \simeq 500$ km/GeV for $|\Delta m^2_{32}| = 2.5 \times 10^{-3}$ eV^2 [88]. To study oscillations in this region, one has to require that the energy of the "first-maximum" be smaller than the MSW resonance energy: $2\sqrt{2}G_{\rm F} n_e E_\nu^{\max} \lesssim \Delta m^2_{32} \cos 2\theta_{13}$. This fixes a limit on the baseline $L_{\max} \approx$5000 km beyond which matter effects spoil the sensitivity.

As an example, Fig. 14 shows the sensitivity on the CP violating phase δ for two concrete cases. We have classified the events in the five categories previously mentioned, assuming an electron charge confusion of 0.1%. We have computed the exclusion regions in the $\Delta m^2_{12} - \delta$ plane fitting the visible energy distributions, provided that the electron detection efficiency is $\sim$ 20%. The excluded regions extend up to values of $|\delta|$ close to π, even when θ_{13} is left free.

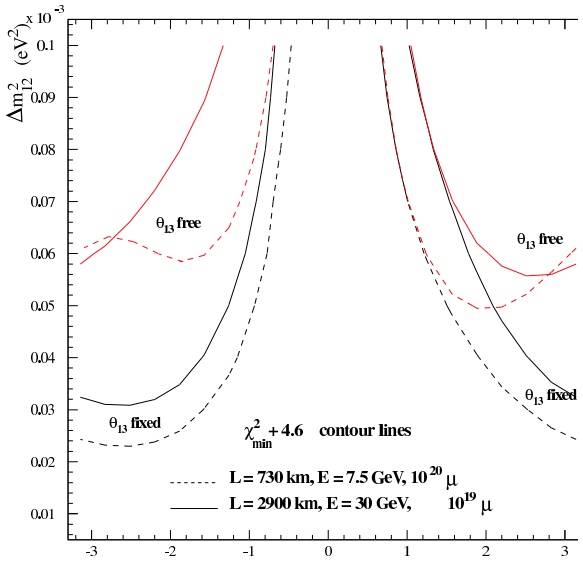

Fig. 14. GLACIER 90% C.L. sensitivity on the CP-phase δ as a function of Δm^2_{21} for the two considered baselines. The reference oscillation parameters are $\Delta m^2_{32} = 3 \times 10^{-3}$ eV^2, $\sin^2\theta_{23} = 0.5$, $\sin^2\theta_{12} = 0.5$, $\sin^2 2\theta_{13} = 0.05$ and $\delta = 0$. The lower curves are made fixing all parameters to the reference values while for the upper curves θ_{13} is free.

4. Summary

It is fair to say that large underground detectors, conceived to search for proton decay, an unavoidable prediction of grand unified theories, have given birth to astroparticle physics through the spectacular detection of Supernova 1987a through neutrinos and the cosmic ray and solar anomalies in the neutrino sector at the origin of the discovery and/or confirmation of the neutrino oscillations. The present review has hopefully shown the ways the proposed detectors will increase by one or two orders of magnitude the observation sensitivities and the discovery potential of the above program. The proposed detectors also present a rich set of complementary aspects:

- In general MEMPHYS profits from large statistics, while GLACIER profits from good pattern recognition and LENA from low energy threshold.
- MEMPHYS and LENA are good in anti-neutrino detection while GLACIER is good on neutrino detection. Both neutrinos and antineutrinos are needed for an in-depth study of supernovae.
- MEMPHYS has complementary sensitivity to LENA/GLACIER on proton decay flavor signatures.

A brief summary of the scientific case for non-accelerator topics is presented in Table VIII.

The proponents of these large underground technologies are aware of their common and complementary physics potential. They are further aware of the synergies that can result from a common R&D on the following topics:

- Underground Laboratories for very large detectors: best strategies for excavation, access and equipments (rock/salt quality, ventilation, air-conditioning, power supply, *etc.*).
- Safety optimization in Very Large Underground Facilities.
- Technical feasibility and safety of large underground liquid containers (tanker).
- Development of large scale liquid purification systems.
- Development of low-cost photo-sensors for Čerenkov and scintillation processes in optical and DUV regions, of different types (vacuum or gaseous).
- Development of solutions for low-cost readout electronics for a large number of channels and large scale acquisition systems.

Last but not least, a great advantage of large underground detectors is that they concern both non-accelerator/astroparticle physics and neutrino accelerator physics. As it was shown in a previous section, in case DOUBLE-CHOOZ and/or T2K-phase 1 around 2010–2011 have hints of oscillation (that is $\sin^2\theta_{13}$ larger than 1–2%) the Fréjus-CERN beam, in conjunction with one or a combination of the 3 proposed schemes, is the fastest way to explore CP violation. In the opposite case one has to gauge the options of:

- gaining 1.5–2 orders of magnitude on $\sin^2\theta_{13}$ and almost 1 order of magnitude of CP violation search, with a betabeam/superbeam+large underground setup (*e.g.* MEMPHYS and/or LENA), also profiting from its advantages for proton decay and astroparticle physics;
- gaining 3 orders of magnitude one $\sin^2\theta_{13}$ and 2 orders on CP violation physics with a neutrino factory scheme. The choice of GLACIER would then permit to guarantee the neutrino beam potential while also keeping the astroparticle physics sensitivities.

A next generation large underground facility seems therefore an inevitable step for astroparticle and neutrino-beam physics. The question of when and where will have to await scientific input from LHC and the current neutrino program as well as world-wide decisions on the regional location of the next generation of large scale facilities for particle and astroparticle physics. A decision expected at the turn of the next decade. Meanwhile, the European community of large scale underground detectors prepare the physics and technological case in common proposals to the European Union and in good collaboration with other regional (American and Asian) efforts.

TABLE VIII

Brief summary of the physics potential of the proposed detectors for non-accelerator based topics. The (*) stands for the case where one MEMPHYS shaft is filled with gadolinium.

Topics	**GLACIER** (100 kt)	**LENA** (50 kt)	**MEMPHYS** (440 kt)
	Proton decay		
$e^+\pi^0$	0.5×10^{35}	—	1.0×10^{35}
$\bar{\nu}K^+$	1.1×10^{35}	0.4×10^{35}	0.2×10^{35}
	SN ν (10 kpc)		
CC	$2.5 \times 10^4(\nu_e)$	$9.0 \times 10^3(\bar{\nu}_e)$	$2.0 \times 10^5(\bar{\nu}_e)$
NC	3.0×10^4	3.0×10^3	—
ES	$1.0 \times 10^3(e)$	$7.0 \times 10^3(p)$	$1.0 \times 10^3(e)$
DSN ν (5 yrs Sig./Bkgd)	60/30	10-115/4	43-109/47 (*)
Solar ν (1 yr Sig.)	$4.5 \times 10^4/1.6 \times 10^5$ (^{8}B ES/Abs)	$2.0 \times 10^6/7.7 \times 10^4/360$ (^{7}Be/*pep*/^{8}B)	1.1×10^5 (^{8}B ES)
Atmospheric ν (1 yr Sig.)	1.1×10^4	TBD	4.0×10^4 (1-ring only)
Geo ν (1 yr Sig.)	below threshold	≈ 1000	need 2 MeV threshold
Reactor ν (1 yr Sig.)	TBD	1.7×10^4	6.0×10^4 (*)
Dark Matter 10 yrs Sig.	3 events ($\sigma_{\rm ES} = 10^{-4}$,$M > 20$ GeV)	TBD	TBD

REFERENCES

[1] K. Hirata *et al.* (KAMIOKANDE-II Collaboration), *Phys. Rev. Lett.* **58**, 1490 (1987).

[2] K.S. Hirata *et al.*, *Phys. Rev.* **D38**, 448 (1988).

[3] M. Aglietta *et al.*, *Europhys. Lett.* **3**, 1321 (1987).

[4] R.M. Bionta *et al.*, *Phys. Rev. Lett.* **58**, 1494 (1987).

[5] K.S. Hirata *et al.*, *Phys. Rev. Lett.* **63**, 16 (1989).

[6] K.S. Hirata *et al.*, *Phys. Lett.* **B205**, 416 (1988).

[7] Y. Fukuda *et al.*, *Phys. Rev. Lett.* **81**, 1562 (1998)

[8] Q.R. Ahmad *et al.*, *Phys. Rev. Lett.* **89**, 011301 (2002).

[9] E. Aliu *et al.*, *Phys. Rev. Lett.* **94**, 081802 (2005).

[10] The KAMLAND Collaboration *Phys. Rev. Lett.* **94**, 081801 (2005).

[11] `http://www-numi.fnal.gov/`

[12] A. Rubbia, `hep-ph/0402110, hep-ph/0407297`; A. Ereditatio, A. Rubbia, `hep-ph/0409143`.

[13] L. Oberauer, F. von Feilitzsch, W. Potzel, *Nucl. Phys.* B *(Proc. Suppl.)* **138** 108 (2005).

[14] T.M. Undagoitia *et al.*, *Phys. Rev.* **D72**, 075014 (2005) [`hep-ph/0511230`].

[15] A. de Bellefon *et al.*, MEMPHYS: A Large Scale Water Čerenkov Detector at Fréjus, Contribution to the CERN Strategic Committee.

[16] S. Amerio *et al.* (ICARUS Collaboration), *Nucl. Instrum. Methods Phys. Res.* **A527**, 329 (2004).

[17] S. Schoenert *et al.* (BOREXINO Collaboration) `physics/0408032`.

[18] M. Wurm, Diploma thesis 2005.

[19] C.K. Jung, *AIP Conf. Proc.* **533**, 29 (2000) [`hep-ex/0005046`].

[20] K. Nakamura, *Int. J. Mod. Phys.* **A18**, 4053 (2003); Y. Itow *et al.*, The JHF-Kamioka Neutrino Project, `hep-ex/0106019`; M. Ishitsuka, T. Kajita, H. Minakata, H. Nunokawa, *Phys. Rev.* **D72**, 033003 (2005) [`hep-ph/0504026`].

[21] J.F. Beacom, M.R. Vagins, *Phys. Rev. Lett.* **93**, 171101 (2004), `hep-ph/0309300`.

[22] P. Nath, P. Fileviez Pérez, `hep-ph/0601023`, submitted to *Phys. Rep.*

[23] I. Dorsner, P. Fileviez Pérez, *Phys. Lett.* **B625**, 88 (2005) [`hep-ph/0410198`].

[24] H. Georgi, S.L. Glashow, *Phys. Rev. Lett.* **32**, 438 (1974).

[25] I. Dorsner, P. Fileviez Pérez, *Nucl. Phys.* **B723**, 53 (2005) [`hep-ph/0504276`]; I. Dorsner, P. Fileviez Pérez, R. Gonzalez Felipe, `hep-ph/0512068`.

[26] D.G. Lee, R.N. Mohapatra, M.K. Parida, M. Rani, *Phys. Rev.* **D51**, 229 (1995) [`hep-ph/9404238`].

[27] H. Murayama, A. Pierce, *Phys. Rev.* **D65**, 055009 (2002) [hep-ph/0108104]; B. Bajc, P. Fileviez Pérez, G. Senjanovic, *Phys. Rev.* **D66**, 075005 (2002) [hep-ph/0204311]; B. Bajc, P. Fileviez Pérez, G. Senjanovic, hep-ph/0210374; D. Emmanuel-Costa, S. Wiesenfeldt, *Nucl. Phys.* **B661**, 62 (2003) [hep-ph/0302272].

[28] K.S. Babu, R.N. Mohapatra, *Phys. Rev. Lett.* **70**, 2845 (1993) [hep-ph/9209215]; C.S. Aulakh, B. Bajc, A. Melfo, G. Senjanovic, F. Vissani, *Phys. Lett.* **B588**, 196 (2004) [hep-ph/0306242]; T. Fukuyama, A. Ilakovac, T. Kikuchi, S. Meljanac, N. Okada, *J. High Energy Phys.* **0409**, 052 (2004) [hep-ph/0406068]; H.S. Goh, R.N. Mohapatra, S. Nasri, S.P. Ng, *Phys. Lett.* **B587**, 105 (2004) [hep-ph/0311330].

[29] T. Friedmann, E. Witten, *Adv. Theor. Math. Phys.* **7**, 577 (2003) [hep-th/0211269].

[30] S. Agostinelli *et al.* (Geant4 Collaboration), *Nucl. Instrum. Methods Phys. Res.* **A506**, 250 (2003).

[31] T. Hayaka, *Nucl. Phys. B (Proc. Suppl.)* **138**, 376 (2005).

[32] K. Kobayashi *et al.* (Super-Kamiokande Collaboration), *Phys. Rev.* **D72**, 052007 (2005) [hep-ex/0502026].

[33] A.S. Dighe, A.Y. Smirnov, *Phys. Rev.* **D62**, 033007 (2000).

[34] L. Cadonati *et al.*, *Astropart. Phys.* **16**, 361 (2002), hep-ph/0012082.

[35] J.F. Beacom *et al.*, *Phys. Rev.* **D66**, 033001 (2002) [hep-ph/0205220].

[36] G.L. Fogli, E. Lisi, A. Mirizzi, D. Montanino, *JCAP* **0504**, 002 (2005).

[37] M. Kachelriess, R. Tomas, R. Buras, H.T. Janka, A. Marek, M. Rampp, *Phys. Rev.* **D71**, 063003 (2005).

[38] I. Gil-Botella, A. Rubbia, *JCAP* **0408**, 001 (2004) [hep-ph/0404151].

[39] I. Gil-Botella, A. Rubbia, *JCAP* **0310**, 009 (2003).

[40] R.C. Schirato, G.M. Fuller, astro-ph/0205390.

[41] G.L. Fogli, E. Lisi, D. Montanino, A. Mirizzi, *Phys. Rev.* **D68**, 033005 (2003).

[42] R. Tomas, M. Kachelriess, G. Raffelt, A. Dighe, H.T. Janka, L. Scheck, *JCAP* **0409**, 015 (2004).

[43] V. Barger, P. Huber, D. Marfatia, *Phys. Lett.* **B617**, 167 (2005).

[44] C. Lunardini, A.Yu. Smirnov, *Nucl. Phys.* **B616**, 307 (2001).

[45] A.S. Dighe, M.T. Keil, G.G. Raffelt, *JCAP* **0306**, 006 (2003).

[46] A.S. Dighe, M.T. Keil, G.G. Raffelt, *JCAP* **0306**, 005 (2003).

[47] C. Lunardini, A.Y. Smirnov, *JCAP* **0306**, 009 (2003).

[48] R. Tomas, D. Semikoz, G.G. Raffelt, M. Kachelriess, A.S. Dighe, *Phys. Rev.* **D68**, 093013 (2003).

[49] P. Antonioli *et al.*, *New J. Phys.* **6**, 114 (2004).

[50] A. Odrzywolek, M. Misiaszek, M. Kutschera, *Astropart. Phys.* **21**, 303 (2004).

[51] S. Ando, J.F. Beacom, H. Yuksel, *Phys. Rev. Lett.* **95**, 171101 (2005) [astro-ph/0503321].

[52] M. Fukugita, M. Kawasaki, *Mon. Not. Roy. Astron. Soc.* **340**, L7 (2003).

[53] S. Ando, *Phys. Lett.* **B570**, 11 (2003).

[54] G.L. Fogli, E. Lisi, A. Mirizzi, D. Montanino, *Phys. Rev.* **D70**, 013001 (2004).

[55] M. Malek, *et al.* (Super-Kamiokande Collaboration), *Phys. Rev. Lett.* **90**, 061101 (2003) [hep-ex/0209028].

[56] S. Ando, *Astrophys. J.* **607**, 20 (2004).

[57] T. Totani, K. Sato, H.E. Dalhed, J.R. Wilson, *Astrophys. J.* **496**, 216 (1998).

[58] T.A. Thompson, A. Burrows, P. Pinto, *Astrophys. J.* **592**, 434 (2003).

[59] M. Keil, G.G. Raffelt, H.T. Janka, *Astrophys. J.* **590**, 971 (2003).

[60] H. Yuksel, S. Ando, J.F. Beacom, astro-ph/0509297.

[61] A.G. Cocco, A. Ereditato, G. Fiorillo, G. Mangano, V. Pettorino, *JCAP* **0412**, 002 (2004) [hep-ph/0408031].

[62] B. Autin, *et al.*, CERN-2000-012.

[63] J.J. Gomez-Cadenas *et al.*, CERN working group on Super Beams (2001), hep-ph/0105297.

[64] A. Blondel *et al.*, *Nucl. Instrum. Methods Phys. Res.* **A503**, 173 (2001).

[65] M. Mezzetto, *J. Phys. G* **29**, 1781 (2003) [hep-ex/0302005].

[66] M. Apollonio *et al.*, hep-ph/0210192.

[67] J.-E. Campagne, A. Cazes, *Eur. Phys. J.* **C45**, 643 (2006) [hep-ex/0411062].

[68] J.E. Campagne, M. Maltoni, M. Mezzetto, T. Schwetz, hep-ph/0603172, submitted to *Phys. Rev.* **D**.

[69] J.-E. Campagne, hep-ex/0510029.

[70] M.G. Catanesi *et al.* (HARP Collaboration), CERN-SPSC/2001-017 SPSC/P322 May 2001.

[71] M. Maltoni, T. Schwetz, M.A. Tortola, J.W.F. Valle, *New J. Phys.* **6**, 122 (2004) [hep-ph/0405172].

[72] P. Zucchelli, *Phys. Lett.* **B532**, 166 (2002).

[73] M. Mezzetto, *J. Phys. G* **29**, 1771 (2003) [hep-ex/0302007].

[74] J. Bouchez, M. Lindroos, M. Mezzetto, *AIP Conf. Proc.* **721**, 37 (2004) [hep-ex/0310059].

[75] M. Mezzetto, *Nucl. Phys. Proc. Suppl.* **143**, 309 (2005) [hep-ex/0410083].

[76] A. Donini, E. Fernandez-Martinez, P. Migliozzi, S. Rigolin, L. Scotto Lavina, *Nucl. Phys.* **B710**, 402 (2005) [hep-ph/0406132].

[77] J. Burguet-Castell, M.B. Gavela, J.J. Gomez-Cadenas, P. Hernandez, O. Mena, *Nucl. Phys.* **B608**, 301 (2001) [hep-ph/0103258]; H. Minakata, H. Nunokawa, *J. High Energy Phys.* **0110**, 001 (2001) [hep-ph/0108085]; G.L. Fogli, E. Lisi, *Phys. Rev.* **D54**, 3667 (1996) [hep-ph/9604415].

[78] D.S. Ayres *et al.* [NOvA Coll.], hep-ex/0503053.

[79] J. Burguet-Castell, D. Casper, E. Couce, J.J. Gomez-Cadenas, P. Hernandez, *Nucl. Phys.* **B725**, 306 (2005) [hep-ph/0503021].

[80] J. Burguet-Castell, D. Casper, J.J. Gomez-Cadenas, P. Hernandez, F. Sanchez, *Nucl. Phys.* **B695**, 217 (2004) [hep-ph/0312068].

[81] F. Terranova, A. Marotta, P. Migliozzi, M. Spinetti, *Eur. Phys. J.* **C38**, 69 (2004) [hep-ph/0405081].

[82] P. Huber, M. Lindner, M. Rolinec, W. Winter, *Phys. Rev.* **D73**, 053002 (2006) [hep-ph/0506237].

[83] O. Bruning *et al.*, CERN-LHC-PROJECT-REPORT-626.

[84] A. Donini *et al.*, hep-ph/0511134.

[85] M. Lindroos, EURISOL DS/TASK12/TN-05-02 to be published in *Nucl. Phys. Proc. Suppl.* (2006).

[86] A. Badertscher, M. Laffranchi, A. Meregaglia, A. Muller, A. Rubbia, *Nucl. Instrum. Methods Phys. Res.* **A555**, 294 (2005) [physics/0505151].

[87] A. Bueno, M. Campanelli, A. Rubbia, *Nucl. Phys.* **B589**, 577 (2000) [hep-ph/0005007].

[88] A. Bueno, M. Campanelli, S. Navas-Concha, A. Rubbia, *Nucl. Phys.* **B631**, 239 (2002) [hep-ph/0112297].

[89] D. Mei, A. Hime, *Phys. Rev.* **D73**, 053004 (2006) [astro-ph/0512125].